

Sliding Impedance Control for Improving Transparency in Telesurgery

Samim Khosravi, Arash Arjmandi and Hamid D. Taghirad, *Senior Member, IEEE*

Advanced Robotics and Automated Systems (ARAS), Industrial Control Center of Excellence (ICCE),

Faculty of Electrical and Computer Engineering, K.N. Toosi University of Technology, Tehran, Iran.

Email: {S.khosravi, a.arjmandi}@ee.kntu.ac.ir, taghirad@kntu.ac.ir

Abstract—This paper describes a novel control scheme for teleoperation with constant communication time delay and soft tissue in environment of slave side. This control scheme combine fidelity criteria with sliding impedance. Fidelity is a measure for evaluating telesurgical system when environment at slave side contains soft tissues. Sliding impedance is used to stabilize the teleoperating system with constant time delays and improve tracking performance in the presence of uncertainties in slave dynamics. The control system contains impedance and sliding impedance control in master and slave manipulators, respectively. Parameters of sliding impedance controller are obtained from fidelity optimization problem while parameters of master impedance controller are determined such that to guarantee stability of the entire teleoperation system. Simulation results demonstrate suitable performance of position and force tracking of the telesurgical system.

Keywords— *Sliding impedance control, fidelity criteria, telesurgery, soft tissue*

I. INTRODUCTION

MINIMAL invasive surgery (MIS) is a type of surgery in which surgeon makes small incisions on patient's body and lead surgical instruments inside the body through trocar tubes. Among advantages of MIS toward traditional open surgery one may name, reducing recovery period, and pain and blood loss during and after operation. Besides unique benefits of MIS, lack of direct surgeon's accessibility to operation location decreases capability and skills of surgeons for performing operation [2]. Due to such benefits in minimal invasive surgery, tendency to use the robots in MIS has increased in recent years as the robots have greater dexterity in comparison with human hand in small workspace. By this means, surgeon interacts with a master robot and this haptic device controls the slave robot that is performing the surgery on the patient. The overall system is called telesurgery.

Among the advantages of telesurgery one may name, increasing surgeon's skills in operation, improving surgeon posture during surgery, ability to do complicated surgeries that surgeons had already difficulty to perform and capability of surgeon's tremor cancellation. However, one of the major problems in telesurgery is lack of surgeon sense of soft tissues such as vessels, tumors and etc, that should be distinguished during the surgery. To overcome this problem, in this paper fidelity criteria is used as a measure to determine the sensitivity of telesurgery system to changes in soft tissue impedance [3].

There are other methods to discriminate soft tissue during the surgery such as adaptive estimation of environment impedance [14], performance metrics for kinesthetic perception [12].

In recent decades, telesurgery is used in many surgeries such as Orologi, Laparoscopic, cardiac and etc. Eye surgeons recently want to use robotic surgery and telesurgery for accomplishing surgery because of difficulties that are faced during operation. Some of issues one may name, lack of suitable working space in traditional surgery, hand tremor that occur in handling surgery instruments, especially for novice surgeons, inaccessibility to the inside eye such as retinal, vitreous and etc. Such problems in eye surgery has caused surgeons may be interested to use robotic in their operations. When robots enter to eye surgeries, using a haptic device as master robot and telesurgery can help to surgeon to improve his/her performance during eye surgery.

In recent years, many attempts has been done to build appropriate robots for eye surgery. First structure of eye robot surgery which was invented in 1989 and introduced in [8]. This robot can be used in vitrectomy and spherical kratotomy eye surgeries. In 1998, Robotic ocular ultra-microsurgery was fabricated by YU and Cringle which is used for delivering drug to eye's inside [5]. First eye robot surgery that used in telesurgery system is the Robot Assisted Microsurgery system which is made by Charles in 1997 [13]. In 2006, famous DaVinci robot surgery was used in eye surgery for the first time. The robot is utilized for suturing the sclera of the eye, cataract surgery and vitrectomy. However, due to problems with force feedback performance and special structure of the robot in surgeries [13], the use of DaVinci in eye surgery did not extend. Recently, UCLA university in cooperation with Stein Jules ophthalmology institute have tried to construct the eye telesurgery system that is called Intraocular Robotic Interventional Surgery System (IRISS). This robot is similar to SMOS structure but it can significantly cancel surgeon's hand tremor by software filter and position scaling between master and slave robot. In 2011, Thins designed and fabricated an especial robot for operation on retina and vitreous of eye [10]. Since spherical workspace is necessary in cataract surgery for cutting sclera of the eye, SMOS is chosen in this paper. In this paper, impedance control and sliding impedance control is used in master and slave side of telesurgery system, respectively. Cho and et al used this control scheme in one DOF

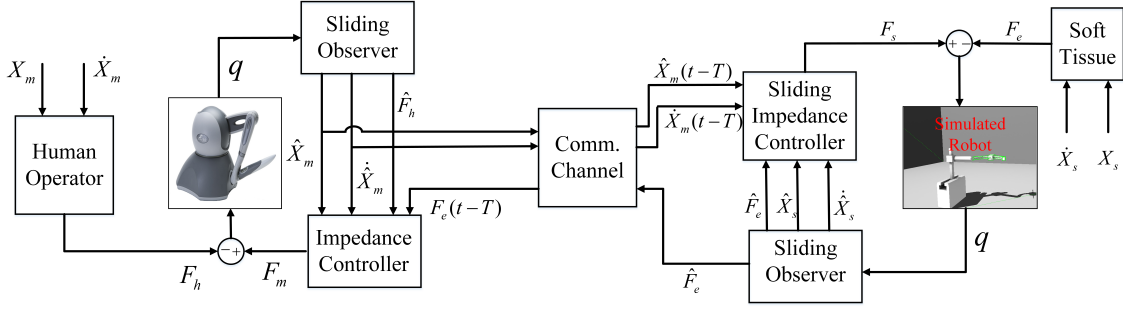


Fig. 1: Overall telesurgery system

teleoperation system under time varying delay [4]. Garcia et al utilized higher order sliding impedance control for one DOF master-slave robot in the presence constant time delay [7]. In this article, a linear observer is designed to replace velocity and acceleration measurement. Furthermore, this control scheme has been extended to n-DOF manipulators by Daly and et al [6], in which a sliding mode observer is used to estimate velocity and external force of each subsystem.

In all previous papers, performance of system has been studied in hard contact situation and the main focus is just to stabilize the entire system. However, the proposed control scheme in this paper combines sliding impedance control with fidelity criteria that is a performance measure for interacting with soft tissues. Contribution of this paper is the way to determine sliding impedance controller parameters in order for the performance criteria of the system is optimized in presence of soft tissue environment with constant time delay in communication channel. In addition, sliding mode observer has utilized for estimation of external force in presence of communication time delay in the system.

II. PRELIMINARIES

Teleoperation system consists of three components, namely master and slave manipulators and the communication channel. Structure of this system with proposed control scheme is illustrated in figure 1. These components are described in the following subsections.

A. Master and Slave Manipulators

The master manipulator used in our telesurgery system is a Sensable Omni haptic device, whose first three DOF is used in the operation. Slave manipulator is SMOS¹ which is proposed for ocular surgery [8]. Although, in this paper all the dynamics of robots and entire teleoperation system have been simulated by MATLAB but slave robot has already been implemented as a virtual reality [1]. Therefore, implementation of the proposed control scheme in this article is the future work of this research.

The joint space dynamics of this manipulators can be generally represented by following differential equation:

$$M_i(q_i)\ddot{q}_i + C_i(q_i, \dot{q}_i)\dot{q}_i + G_i(q_i) = \tau_i + J^T F_{ext}, \quad (1)$$

where $M_i(q)$, $C_i(q, \dot{q})$, $G_i(q)$ and τ_i are inertia matrix, Coriolis and centrifugal matrices, gravity vector and torque control effort, respectively. Also, $i \in \{\text{master}, \text{slave}\}$ and J is Jacobian matrix.

Details of master manipulator dynamic has been discussed in [11], and is not described in detail in this paper. Slave robot of the telesurgery system is illustrated in Figure 2. This robot has five DoFs whose first two DoFs set position of the robot end effector on patient head and the other DoFs provide a spherical workspace on patient's eye. Dynamic equations of this robot have been derived using Lagrange method for the last three DoFs, and the resulting dynamic matrices are given in Appendix A.

For applying the impedance controllers, dynamic equations may be written in Cartesian space as follows:

$$\tilde{M}_i(x_i)\ddot{x}_i + \tilde{C}_i(x_i, \dot{x}_i)\dot{x}_i + \tilde{G}_i(x_i) = F_i + F_{ext}, \quad (2)$$

where

$$\begin{aligned} \tilde{M}(x_i) &= (J_i^T(q_i))^{-1} M_i(q_i) J_i(q_i)^{-1}, \\ \tilde{C}(x_i, \dot{x}_i) &= (J_i^T(q_i))^{-1} C_i(q_i, \dot{q}_i) - \tilde{M}(x_i) \dot{J}_i(q_i) \dot{q}_i \\ \tilde{G}(x_i) &= J_i^T(q_i) G(q_i) \end{aligned}$$

B. Communication Channel

Structure of bilateral teleoperation system used in this research is direct force reflection (DFR) and utilizes a communication channel for transmitting position and force signals between master and slave subsystems. The communication

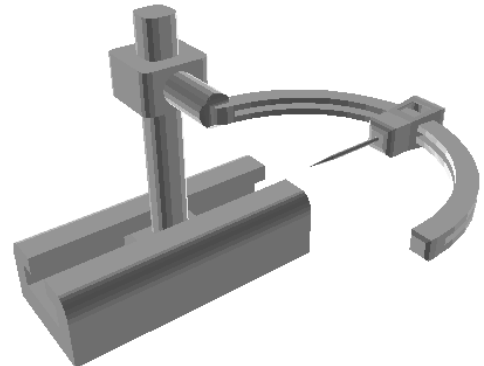


Fig. 2: Slave robot in telesurgery system

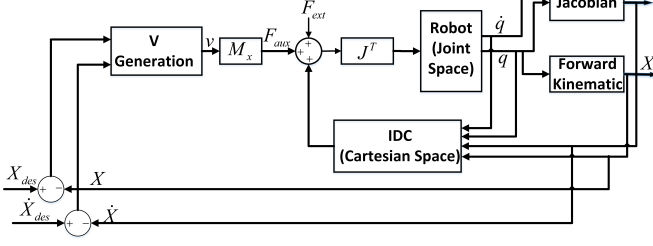


Fig. 3: Control Diagram used in each subsystems

channel may be subject to time delays and data losses. In this paper, time delays in communication channel are assumed to be constant and data loss are neglected. In this case, the communication channel can be presented by,

$$\begin{aligned} x_s(t) &= x_m(t - T) \\ F_{em}(t) &= F_e(t - T). \end{aligned} \quad (3)$$

where x_s and x_m are position of slave and master subsystem, respectively. F_{em} is reflected environment force to master side. T is the communication time delay that is considered to be constant and identical for both channels.

III. TELEOPERATION CONTROL SYSTEM

In the proposed control scheme, an impedance controller is used for master manipulator in order to provide the operator with the sense of remote environment. For the slave side, however, a sliding mode impedance controller is used which is able to compensate the uncertainties in the manipulator dynamics since the model of slave robot is more uncertain than that of the master robot.

For the master side, the impedance controller is designed so as to guaranty the stability of the teleoperating system, while sliding mode controller for the slave subsystem is designed in such a way to optimize fidelity of the overall system. Structure of the proposed scheme in both subsystems are similar and is illustrated in Figure 3. As it is seen in this figure, Jacobian and forward kinematics are used for taking Cartesian variables of robot, and therefore, it is necessary to make the assumption that both manipulators operate in their singular-free workspaces. At each side, inverse dynamic in Cartesian space is demanded for applying impedance control. In the following subsection, we discuss on how to achieve the v signal in Fig. 3

A. Master Controller

On the master side, impedance controller is used for reflecting environment force to master. The desired impedance for master robot is selected as

$$\bar{M}_m \ddot{X}_m(t) + \bar{B}_m \dot{X}_m(t) + \bar{K}_m X_m(t) = F_h(t) - F_e(t - T), \quad (4)$$

where \bar{M}_m , \bar{B}_m , \bar{K}_m denote desired inertia, damping and spring coefficient matrices of master manipulator, respectively. It should be noted that environment force is reflected to the master robot through the communication channel to be sensed

by human operator. These parameters are held in a manner that stability of a teleoperation system is maintained [6]. Such values may be given as following:

$$\begin{aligned} m_m &> \sqrt{\frac{3}{2}} \|G_s\|_\infty, k_m = m_m, b_m = \sqrt{k_m m_m} \\ \bar{M}_m &= \bar{K}_m = \text{diag}\{m_m, m_m, m_m\} \\ \bar{B}_m &= \text{diag}\{b_m, b_m, b_m\}, \end{aligned} \quad (5)$$

In which, G_s is the transfer function matrix of slave with environment system impedance, and therefore, environment force and velocity error between master and slave are chosen as output and inputs of the system, respectively. Finally, based on what is said, signal v of master controller can be obtained as

$$v = \bar{M}_m^{-1} \left(\bar{B}_m \dot{X}_m(t) + \bar{K}_m X_m(t) - F_h(t) + F_e(t - T) \right) \quad (6)$$

where J and \tilde{M}_m are Jacobian and inertia matrix in Cartesian space, respectively.

B. Slave Controller

On the slave side, sliding mode structure based on impedance control is applied for tracking the master position by slave robot in the presence of uncertainty in slave robot dynamics. Sliding surface of slave controller may be defined as

$$s = \int_0^t \bar{M}_s I(\tau) d\tau, \quad (7)$$

where I denotes the desired impedance of slave robot and may be considered as

$$I = \bar{M}_s \ddot{e} + \bar{B}_s \dot{e} + \bar{K}_s e - F_e. \quad (8)$$

As introduced in (8), position error between master and slave is represented by $e = X_s(t) - X_m(t - T)$. Also, F_e denotes the environment force. The desired impedance parameters are chosen by fidelity criteria optimization problem. Fidelity measure is a performance criteria when in teleoperation system the environment consists of soft tissues. This optimization problem may consider robust stability constraint to guarantee robustness of teleoperation system against variation in environmental impedance at slave side. Thus, Fidelity optimization problem is formulated as follows:

$$\arg \sup_{\text{Robust Stability}} (\text{fidelity criteria}) \quad (9)$$

If the teleoperation system is considered as a two-port network, then its hybrid matrix can be expressed as

$$\begin{bmatrix} F_h(s) \\ V_s(s) \end{bmatrix} = \begin{bmatrix} h_{11} & h_{12} \\ h_{21} & h_{22} \end{bmatrix} \begin{bmatrix} V_m(s) \\ -F_e(s) \end{bmatrix} \quad (10)$$

in which,

$$\begin{aligned} h_{11} &= \bar{m}_m s + \bar{b}_m + \frac{\bar{k}_m}{s} \\ h_{12} &= -h_{21} = -e^{-Ts} \\ h_{22} &= \frac{s}{\bar{m}_m s^2 + \bar{b}_m s + \bar{k}_s} \end{aligned} \quad (11)$$

Note that above hybrid matrix was written in one direction and all parameters in formula are scalars. Then the cost function of fidelity measure may be given by

$$J = \left\| W_s \frac{dZ_t}{dZ_e} \Big|_{Z_e=\hat{Z}_e} \right\|_2 = \left\| W_s \frac{-h_{12}h_{21}}{(1+h_{22}\hat{Z}_e)^2} \right\|_2 \quad (12)$$

Where W_s denotes the weighting function which is obtained from experimental results and \hat{Z}_e is nominal environment impedance. According to cost function formulation 12, fidelity measure optimizes sensitivity function of transmitted impedance to environment impedance. In order to guarantee robust stability of the system, the constraint of this optimization problem is formulated as follows:

$$\|W_u T\|_\infty < 1, \quad (13)$$

where W_u denotes the uncertainty weighting function which is achieved from changes in impedance of the environment, while T denotes the closed loop transfer function of teleoperation system [9]. Finally, fidelity optimization problem is formulated as following.

$$\arg \sup_{\|W_u T\|_\infty < 1} \left\| W_s \frac{-h_{12}h_{21}}{(1+h_{22}\hat{Z}_e)^2} \right\|_2. \quad (14)$$

Notice that the desired impedance parameters may be considered in the diagonal matrix form, and therefore, identical in all three directions. Hence, this problem has three variables to be found by optimization solution. For the sake simplicity and in order to force the tracking error to a desired shape, it is proposed to choose the variables of optimization as following.

$$m_s = 1, \quad b_s = 2\zeta\omega_n, \quad k_s = \omega_n^2, \quad (15)$$

in which, ζ is set to 0.707 for a desired shape of tracking error, and ω_n is the only parameter remains in the optimization problem. Notice that the tracking performance considered in [3] is an extra constraint taken into account after the optimization is performed. However, in what we proposed, this enters directly in the optimization problem to obtain the controller parameters. Therefore, it is expected to obtain more suitable tracking performance by this means. Furthermore, through this formulation time delay appear just inside the closed loop transfer function of system and do not affect on cost function due to the structure of this optimization problem. Hence, Pade approximation may be used in the closed loop transfer function in order to solve the optimization problem in a tractable fashion. Incorporating these note, the v signal can be attained as follows:

$$v = \bar{M}_s^{-1} \left(\bar{B}_s (\dot{\mathbf{X}}_m(t-T) - \dot{\mathbf{X}}_s(t)) + \bar{K}_m (\mathbf{X}_m(t-T) - \mathbf{X}_s(t)) - \mathbf{F}_e(t) \right) + \left(\bar{M}_m^{-1} \left(\bar{B}_m \dot{\mathbf{X}}_m(t-T) + \bar{K}_m \mathbf{X}_m(t-T) + \mathbf{F}_h(t-T) - \mathbf{F}_e(t-2T) \right) \right) + K_g \text{sign}(s) \quad (16)$$

where K_g is the sliding coefficient and T is the time delay value in communication channel.

IV. SLIDING MODE OBSERVER

As mentioned in previous sections, external forces such as environment and human interaction forces shall be used in the proposed control scheme. Therefore, if such measurements are unavailable due to sterilize surgical instruments or expensive to be applied, force estimation may be used as an alternative. In this paper, sliding mode observer is used to estimate external forces. This scheme is widely used in mechanical systems because of its finite time convergence property, robustness to model uncertainty and ability to estimate unknown input signals. Finite time convergence property of sliding observer makes it suitable to replace actual variables in the analysis of system. Observer dynamics are as follow:

$$\begin{aligned} \dot{\hat{\mathbf{x}}}_1 &= \hat{\mathbf{x}}_2 + \mathbf{z}_1, \\ \dot{\hat{\mathbf{x}}}_2 &= M_i(\hat{\mathbf{x}}_1)^{-1} (C_i(\hat{\mathbf{x}}_2, \hat{\mathbf{x}}_1) + G_i(\hat{\mathbf{x}}_1)) + \mathbf{z}_2, \end{aligned} \quad (17)$$

where,

$$\begin{aligned} \mathbf{z}_1 &= \alpha_i |\mathbf{x}_1 - \hat{\mathbf{x}}_1|^{\frac{1}{2}} \text{sign}(\mathbf{x}_1 - \hat{\mathbf{x}}_1), \\ \mathbf{z}_2 &= \lambda_i \text{sign}(\mathbf{x}_1 - \hat{\mathbf{x}}_1). \end{aligned} \quad (18)$$

In above equations, x_1 denotes measured joint angle of the robot and \hat{x}_1, \hat{x}_2 are estimated joint angle and joint velocity, respectively. α_i and λ_i are observer parameters that are calculated based on uncertainty in dynamic model for regulating rate of reaching estimated values to real ones. Note that joint space variables of robot dynamic are estimated through the observer while in control scheme, Cartesian variables are used so forward kinematic and Jacobian should be used for estimating Cartesian variables. External forces estimation at each side may be obtained as follows:

$$\mathbf{F}_{ext} = J_i^T M_i(\mathbf{x}_1) \mathbf{z}_2 \quad ; \quad i \in \{\text{master, slave}\}, \quad (19)$$

where J is Jacobian matrix correspond to each robot.

V. SIMULATION RESULTS

For simulation of telesurgery system, master and slave robot dynamics is simulated in MATLAB and these robots are connected through a communication channel with a constant delay block. Because one of the actions which is performed in cataract eye surgery is cutting the cornea on circular track, such trajectory is considered in the telesurgery simulation. In order to generate such trajectory consider:

$$x = 0.05 \sin(t), z = 0.05 \cos(t), y = 0.03, \quad (20)$$

Note that masters end-effector is rotated in xz plane and 3cm upward of its reference frame. Parameters which is used in the simulation are shown in table I.

Sign functions in equation (18) are replaced with tangent hyperbolic function to have smoother and faster simulations. Maximum step size in simulations is set to 2×10^{-5} and $\pm 30\%$ uncertainty is considered in the mass of the links of slave manipulator.

TABLE I: Simulation Parameters

Parameters	Value
λ	200
α	900
\bar{m}_{ds}	1
\bar{b}_{ds}	13.77
\bar{k}_{ds}	94.93
\bar{m}_{dm}	22
\bar{b}_{dm}	32
\bar{k}_{dm}	22

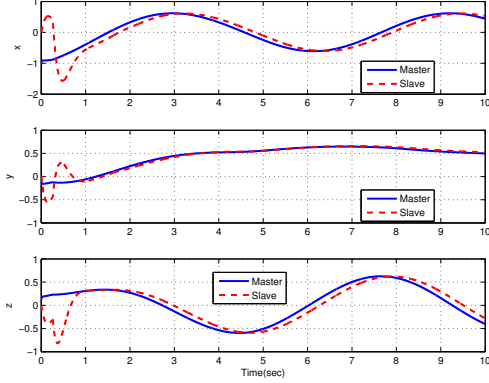


Fig. 4: Position tracking in free motion case

A. Free Motion Results

In free motion case, only position tracking between master and slave is considered. As it can be seen in Fig. 4, the tracking error diminishes as system states converge to the desired sliding surface. Having system converged to sliding surface, system performance is determined by parameters selected for desired impedance. As it is shown in this figure, perfect position tracking is achieved, in the presence of communication time delays. Due to the uncertainties in dynamics model of slave manipulator it requires a finite time for the systems states to converge to the desired sliding surface which is defined in Section III-B. Fig. 5 illustrates evaluation of observer performance. Convergence time in these figures is

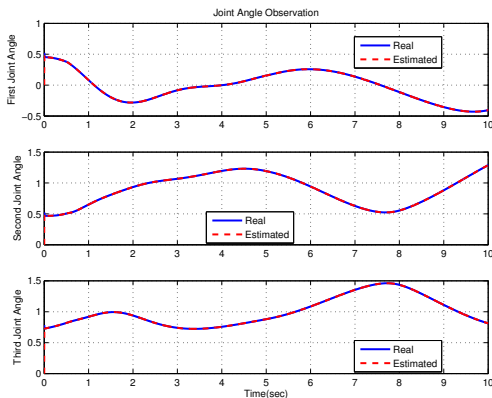


Fig. 5: Estimation of joint angles in master side

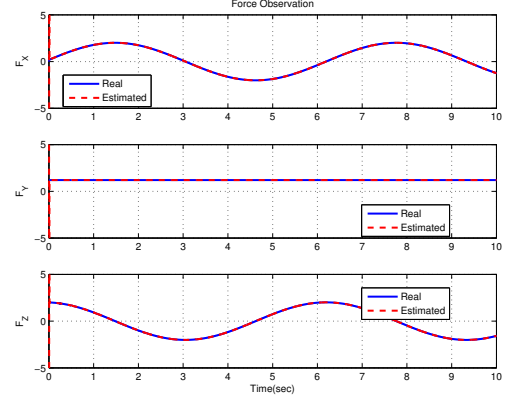


Fig. 6: Estimation of human force in master side

few hundredths of a second. Fig. 6 represents human force as unknown input signal in master robot that is estimated by the observer. As it is seen in this figure, perfect performance is obtained, as expected.

B. Constrained Motion Results

In this case, environment at slave side is modeled as a spring-damper with nominal values are 70 and 50, respectively. In order to obtain uncertainty profile in fidelity stability constraint, these values are changed between zero to infinity as described in [3]:

$$\phi = \frac{1.413 (0.06667 s + 1.0) ((2.066 \cdot 10^{-5}) s^2 + 0.0009091 s + 1.0)}{(0.001 s + 1.0) ((9.07 \cdot 10^{-5}) s^2 + 0.005143 s + 1.0)},$$

$$W_u = \frac{1}{h_{22} Z_e} \phi, \quad (21)$$

in which, h_{22} and Z_e are slave admittance (defined in 10), and nominal environment impedance, respectively.

Fig. 7 shows position tracking in this case. In this figure, end effector of robot is in contact with the soft tissue from beginning and up to 6 seconds. In this period, errors in this position tracking are clearly apparent. The tracking error in this period can be adjusted by tuning the desired impedance parameter. Although the tip of surgical instrument on the SMOS robot has a spherical motion in xz plane but the reflected force to the master is changing due to impedance variation during this trajectory on patient's eye. This verifies that the operator completely feels these variations in environment impedance since fidelity measure of this system is maximized. Fig. 8 shows real and estimated reflected force. As it is shown in this figure, sliding mode observer has suitable performance in this case, as well.

VI. CONCLUSIONS

In recent years, minimal invasive telesurgery is gradually replacing traditional surgeries, however, in this type of surgeries discrimination of soft tissues is still a challenging task. For controlling the telesurgery systems, it is proposed to use impedance control and sliding impedance control in master and slave side, respectively. Parameters of master impedance controller were determined to stabilize the whole system. The slave controller was designed such that to optimizing fidelity

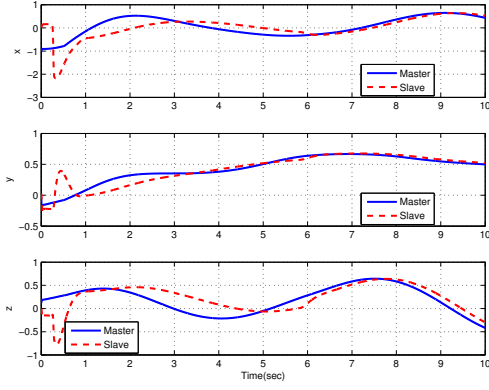


Fig. 7: Position tracking in constrained motion case

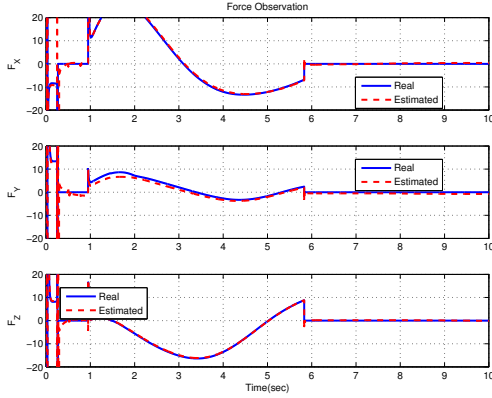


Fig. 8: Environment force estimation

measure and improve surgeon's feeling at manipulating soft tissues during operation. Sliding mode observer was used for estimation of human and environmental force. Simulation results shows promising performance in terms of estimation and control.

REFERENCES

- [1] A. Arjmandi, S. Khosravi, and H. D. Taghirad. Robust peb controller design for teleoperation with variable time delay. In *Control, Instrumentation, and Automation International Conference on*, December 2013.
- [2] I. Font Balaguer. *Haptic feedback control designs in teleoperation systems for minimal invasive surgery*. PhD thesis, Eindhoven: Technische Universiteit Eindhoven, 2004.
- [3] M.C. Cavusoglu, A. Sherman, and F. Tendick. Design of bilateral teleoperation controllers for haptic exploration and telemanipulation of soft environments. *IEEE Transactions on Robotics and Automation*, 18(4):641–647, 2002.
- [4] Hyun-Chul Cho, Jong Hyeon Park, Kyunghwan Kim, and Jong-Oh Park. Sliding-mode-based impedance controller for bilateral teleoperation under varying time-delay. In *Robotics and Automation, 2001. Proceedings 2001 ICRA. IEEE International Conference on*, volume 1, pages 1025–1030 vol.1, 2001.
- [5] Yu DY. Constable IJ, Cringle SJ. Robotic ocular ultramicrosurgery. *Australian and New Zealand Journal of Ophthalmology*, pages 1096–1109, 05 1998.
- [6] J.M. Daly and D.W.L. Wang. Time-delayed output feedback bilateral teleoperation with force estimation for n -dof nonlinear manipulators. *Control Systems Technology, IEEE Transactions on*, 22(1):299–306, Jan 2014.
- [7] L.G. Garcia-Valdovinos, V. Parra-Vega, and M.A. Arteaga. Observer-based higher-order sliding mode impedance control of bilateral teleoperation under constant unknown time delay. In *Intelligent Robots and Systems, 2006 IEEE/RSJ International Conference on*, pages 1692–1699,

- [8] A. Guerrouad and P. Vidal. Smos: stereotaxical microtelemanipulator for ocular surgery. In *Engineering in Medicine and Biology Society, 1989. Images of the Twenty-First Century., Proceedings of the Annual International Conference of the IEEE Engineering in*, pages 879–880 vol.3, 1989.
- [9] Blake Hannaford. Stability and performance tradeoffs in bi-lateral telemanipulation. In *Robotics and Automation, 1989. Proceedings., 1989 IEEE International Conference on*, pages 1764–1767. IEEE, 1989.
- [10] Meenink HCM. *Vitreo-retinal eye surgery robot : sustainable precision*. PhD thesis, Eindhoven: Technische Universiteit Eindhoven, 2011.
- [11] T. Sansanayuth, I. Nilkhamhang, and K. Tungpimolrat. Teleoperation with inverse dynamics control for phantom omni haptic device. In *SICE Annual Conference (SICE), 2012 Proceedings of*, pages 2121–2126, Aug 2012.
- [12] Hyoung Il Son, T. Bhattacharjee, and H. Hashimoto. Enhancement in operators perception of soft tissues and its experimental validation for scaled teleoperation systems. *Mechatronics, IEEE/ASME Transactions on*, 16(6):1096–1109, Dec 2011.
- [13] I. Tsui, A. Tsirbas, C. W. Mango, S. D. Schwartz, and J. P. Hubschman. Robotic surgery in ophthalmology. 2010-01-01.
- [14] X. Wang, P.X. Liu, and Shuyan Wang. Adaptive robust control for bilateral teleoperators in soft environments. In *Mechatronics and Automation, 2005 IEEE International Conference*, volume 4, pages 2055–2060 Vol. 4, July 2005.

APPENDIX

The dynamics of slave robot that has been used in this paper are derived from Lagrange method. The dynamic matrices are given as follow:

$$M_s(q_s) = \begin{bmatrix} M_{11} & M_{12} & 0 \\ M_{21} & M_{22} & 0 \\ 0 & 0 & M_{33} \end{bmatrix},$$

$$V_s(q_s, \dot{q}_s) = [V_1 \quad V_2 \quad V_3]^T,$$

$$G_s(q_s) = [G_1 \quad G_2 \quad G_3]^T,$$

in which, entries of inertia matrix are obtained as follows:

$$M_{11} = 0.009q_3 - 0.007\cos(2q_2) + 4.4 \times 10^{-5}\sin(2q_2) - 0.009q_3\cos(2q_2) - 0.0755q_3^2\cos(2q_2) + 0.0755q_3^2 + 0.0204$$

$$M_{22} = 0.151q_3^2 + 0.0181q_3 + 0.0156$$

$$M_{33} = 0.151$$

$$M_{12} = M_{21} = 1.3 \times 10^{-4} \cos(q_2) + 9.7 \times 10^{-7} \sin(q_2)$$

and Coriolis and centrifugal vector are described in the following form:

$$V_1 = 0.00906\dot{q}_1\dot{q}_3 - 1.3e^{-4}\dot{q}_2^2\sin(q_2) + 9.7 \times 10^{-7}\dot{q}_2^2\cos(q_2) + 0.151\dot{q}_1\dot{q}_3q_3 + 8.8 \times 10^{-5}\dot{q}_1\dot{q}_2\cos(2q_2) + 0.0141\dot{q}_1\dot{q}_2\sin(2q_2) - 0.00906\dot{q}_1\dot{q}_3\cos(2q_2) - 0.151\dot{q}_1\dot{q}_3q_3\cos(2q_2) + 0.0181\dot{q}_1\dot{q}_2q_3\sin(2q_2) + 0.151\dot{q}_1\dot{q}_2q_3^2\sin(2q_2)$$

$$V_2 = 2\dot{q}_2\dot{q}_3(0.151q_3 + 0.00906) - \dot{q}_1^2(0.0755\sin(2q_2)q_3^2 + 0.00906\sin(2q_2)q_3 + 4.4 \times 10^{-5}\cos(2q_2) + 0.00704\sin(2q_2))$$

$$V_3 = -0.00151(50q_3 + 3)(\dot{q}_1^2 - \dot{q}_1^2\cos(2q_2) + 2\dot{q}_2^2)$$

Finally, gravity vector of this robot are derived as:

$$G_1 = 1.12\cos(q_1) + 0.0324\sin(q_1) + 0.00388\cos(q_1)$$

$$\cos(q_2) + 1.27\cos(q_1)\sin(q_2) + 1.48q_3\cos(q_1)\sin(q_2)$$

$$G_2 = 10.2\sin(q_1)(0.116\cos(q_2) - 3.81e^{-4}\sin(q_2))$$

$$+ 1.48\cos(q_2)\sin(q_1)(q_3 + 0.06)$$

$$G_3 = 1.48\sin(q_1)\sin(q_2)$$